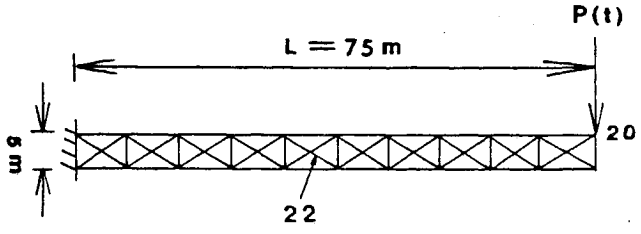

$E = 71.7 \times 10^9$ N/m^2 , $\rho = 2768$ kg/m^3

$c = 4.0 \times 10^8$ N$_s$/m^2 , $L_c = 7.5$ m

$L_g = 5.0$ m , $A_c = 90 \times 10^{-6}$m^2

$A_d = 40 \times 10^{-6}$m^2 , $A_g = 60 \times 10^{-6}$m^2

Fig. 2 Geometry of the cantilevered truss (A_c, A_g, and A_d are the cross-sectional areas of the horizontal, vertical, and diagonal members, respectively).

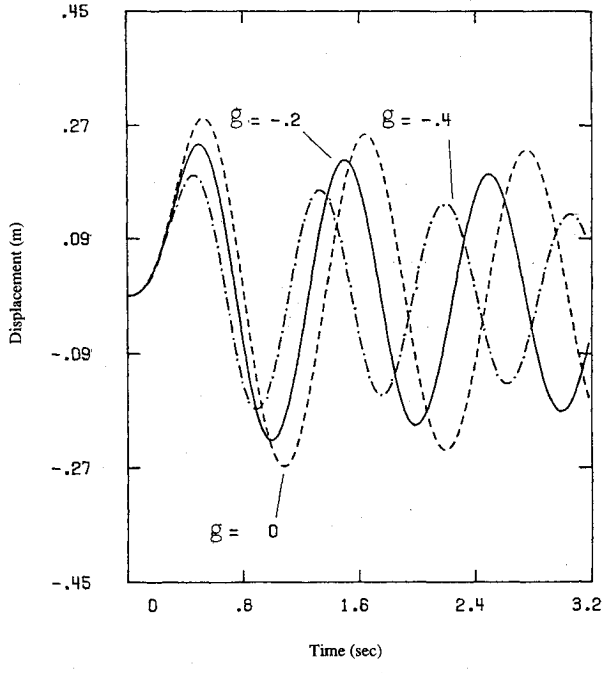

Fig. 3 Transient response history of the vertical displacement at the free tip of the damped structure.

Example

To study the transient forced response with feedback control, a concentrated force is assumed to act at the free tip as shown in Fig. 2. The forcing function is given as

$$P(t) = 100 \sin\left(\frac{\pi t}{T_0}\right) (N) \qquad t \le T_0$$

$$= 0 \qquad t > T_0$$

where $T_0 = 0.5$ s. The transient responses with respect to different gain factors are obtained by using the Newmark finite difference method.[6]

Figure 3 shows the time histories of the vertical displacement at the free tip of the truss with viscous damping. It is evident that with larger negative gains the frequency is increased and the amplitude decreased.

Conclusions

It has been demonstrated that effective structural stiffness and viscous damping can be augmented by the use of an extension-contraction actuator placed in each of the truss members. To achieve this purpose, the gain of the perturbing force of the actuator must be negative.

References

[1]Juang, J. N., "Optimal Design of a Passive Vibration Absorber for a Truss Beam," *Journal of Guidance, Control, and Dynamics,* Vol. 7, No. 6, 1984, pp. 733–739.

[2]Balas, M. J., "Active Control of Flexible Systems," *Journal of Optimization Theory and Applications,* Vol. 25, No. 3, 1978, pp. 415–436.

[3]Aubrun, J. N., "Theory of Control Structures by Low-Authority Controllers," *Journal of Guidance, Control, and Dynamics,* Vol. 3, No. 5, 1980, pp. 444–451.

[4]Meirovitch, L., and Baruch, H., "Control of Self-Adjoint Distributed-Parameter Systems," *Journal of Guidance, Control, and Dynamics,* Vol. 5, No. 1, 1982, pp. 60–66.

[5]Sun, C. T., and Wang, R. T., "Enhancement of Frequency and Damping in Large Space Structures with Extendible Members," *Proceedings of the AIAA/ASME/ASCE/AHS 29th Structures, Structural Dynamics and Materials Conference,* AIAA, Washington, DC, 1988, pp. 1774–1780.

[6]Hughes, T. J. R., and Liu, W. K., "Implicit-Explicit Finite Elements in Transient Analysis: Stability Theory," *Journal of Applied Mechanics,* Vol. 45, No. 2, 1978, pp. 371–374.

Structural Damage Detection Using Modal Test Data

Tae W. Lim*
Lockheed Engineering and Sciences Company, Hampton, Virginia 23666

Introduction

FOR the assessment of structural integrity, the use of system identification techniques has been studied by many investigators.[1-3] Using the system identification techniques, the differences in structural dynamic characteristics between the undamaged and damaged structures are translated into the structural element stiffness changes, which reveal the structural damage. Assuming that the exact measured mode shapes of the damaged structure were available at every finite element degree of freedom (DOF) of the structure, Chen and Garba[1] and Smith and Hendricks[2] investigated the assessment of structural damage. Difficulties in identifying damaged members were reported. The stiffness matrix coefficients corresponding to the undamaged structural members were significantly affected, thereby making the damage detection uncertain. Hajela and Soeiro[3] proposed that static displacement information be incorporated to supplement the flexible modes for damage detection. For large space structures, such as the Space Station Freedom, static deflection may not be available because on-ground assembly testing of these structures is infeasible.

The influence of measurement inaccuracy on the damage detection was not addressed in any of the damage detection techniques described previously. In practice, the measured modes used for the damage detection are corrupted by the measurement noise and the modal parameter identification error. Also, the mode shapes are incomplete, i.e., available only at the measurement locations. This Note presents a systematic method that provides precise identification of the damage location and extent when the exact measured modes at every finite element DOF are used. Also, a procedure is presented to perform a damage detection with inaccurate, incom-

Received July 2, 1990; revision received Nov. 2, 1990; accepted for publication Nov. 9, 1990.

*Senior Engineer, Langley Program Office, 144 Research Drive. Member AIAA.

plete measured modes. The method in this Note is based on the stiffness matrix correction technique using submatrices.[4] The stiffness reduction factor (SRF) for each submatrix, which reveals the location and extent of stiffness damage, is obtained using a computationally efficient pseudoinverse solution. A planar truss example used by Smith and Hendricks[2] is employed to illustrate the method.

Theoretical Development

Minor modifications to the stiffness matrix correction method using submatrices[4] were made to address the structural damage detection problem. The discussion in this Note is limited to only those modifications. To detect the location and extent of damage, the relationship between the individual structural element damage and the changes in the modes needs to be established. To this end, the system stiffness matrix is expanded into a linear sum of submatrices such as

$$[K] = [K_o] + \sum_{j=1}^{p} s_j [K_j] \tag{1}$$

where $[K]$ is the system stiffness matrix, $[K_o]$ the undamaged stiffness matrix, $[K_j]$ the jth submatrix in the global displacement coordinates, s_j the jth SRF, and p the total number of submatrices. The SRF indicates the extent of damage ranging from 0 to -1. No damage and complete loss of stiffness are indicated by $s_j = 0$ and $s_j = -1$, respectively. For damage detection, the individual structural element is represented by a submatrix.

A useful relationship between the submatrices and the modes may be obtained by examining the strain energy of each submatrix with respect to the modes. The fractional modal strain energy distribution among the submatrices, i.e., element stiffness matrices, for mode i can be evaluated by

$$\mathrm{MSE}_{ji} = \frac{\{\phi_i\}^T [K_j] \{\phi_i\}}{\{\phi_i\}^T [M] \{\phi_i\} \omega_i^2} \times 100 \tag{2}$$

where MSE_{ji} is the fractional modal strain energy of the submatrix j in mode i, $[M]$ the system mass matrix, $\{\phi_i\}$ the ith mode shape, and ω_i the ith natural frequency. The submatrices containing a large fraction of modal strain energy for mode i indicate that the structural elements corresponding to the submatrices are major load carrying members for the particular mode. Any damage in those elements will cause significant changes in the frequency and mode shape of the mode; hence, the damage detection using the mode would be possible. On the other hand, the structural elements having a negligible fraction of modal strain energy reflect that the stiffness changes in those members will not produce significant changes in the structural dynamic characteristics. Thus, damage detection in those structural elements using the mode would be difficult. The fractional modal strain energy distribution among structural members for each mode forms a useful indicator in selecting modes for damage detection.

The natural frequencies and mode shapes required for damage detection are obtained through a modal survey. The number of sensors or the test DOF used in the modal survey is typically much smaller than the DOF of the finite element model. The mode shape coefficients are available only at the test DOF and, therefore, damage detection cannot be performed directly with the measured modes. To eliminate this problem, the finite element mass and stiffness matrices and the submatrices are reduced to the test DOF. The reduced representation, often referred to as a test analysis model (TAM), provides a means to perform damage detection using the measured modes directly. Modal reduction[5] is employed to reduce the matrices. The modal reduction method is less restrictive compared to Guyan reduction[6] because a smaller number of test DOF can be used to accurately reduce the finite element model. The measured mode shapes in the test DOF and the measured frequencies are then used to detect changes in the stiffness matrix. The resulting system of linear equations is solved for the SRFs using a pseudoinverse solution. In order to obtain an accurate solution, the product of the number of test DOF and the number of measured modes is required to be greater than or equal to the number of the SRFs to be identified.

Exact detection of the location and extent of damage is possible if proper modes based on the modal strain energy analysis, Eq. (2), are used and the measured modes are exact and available at every finite element DOF. However, the modes obtained from a typical modal survey are inaccurate and incomplete. Also, the TAM generation process induces inaccuracy. Accurate detection of the damage is often hampered by these inaccuracies inherently present in the damage detection process using system identification techniques. Thus, the identified SRFs are not exact and vary depending on the measured mode used and the selected TAM. In order to extract meaningful information under these circumstances, an average SRF weighted by a standard deviation of the SRFs obtained using different sets of modes is proposed. Large standard deviation of SRFs indicates that the SRFs are heavily influenced by the inconsistent measurements. On the other hand, the SRFs with small standard deviation imply that they are generated by the consistent changes of the structural dynamic characteristics in the damaged structure. A weighted average SRF for submatrix j is defined as

$$sw_j = sa_j/\sigma_j \tag{3}$$

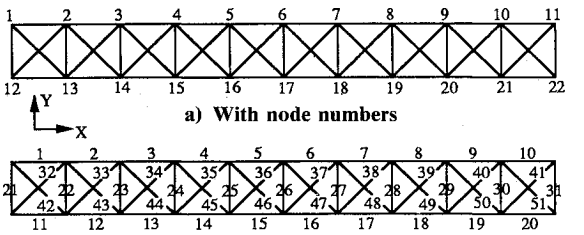

Fig. 1 Ten-bay planar truss.

Table 1 Fractional modal strain energy distribution (%) in the individual truss members of the undamaged structure in the first six flexible modes

Element numbers[a]	Mode number 1	2	3	4	5	6
Longerons (horizontal members)						
1, 10, 11, 20	0.06	0.33	0.27	0.86	1.56	1.05
2, 9, 12, 19	0.91	3.48	1.80	5.95	6.13	5.56
3, 8, 13, 18	3.68	8.10	4.17	5.56	0.67	8.06
4, 7, 14, 17	7.77	6.72	6.50	0.05	2.89	5.15
5, 6, 15, 16	10.85	1.09	7.93	3.71	1.62	0.74
Battens (vertical members)						
21, 31	0.00	0.00	0.01	0.00	0.00	0.04
22, 30	0.00	0.00	0.15	0.00	0.00	0.60
23, 29	0.00	0.00	0.52	0.00	0.00	1.49
24, 28	0.00	0.00	0.96	0.00	0.00	1.43
25, 27	0.00	0.00	1.31	0.00	0.00	0.54
26	0.00	0.00	1.44	0.00	0.00	0.00
Diagonals						
32, 41, 42, 51	0.13	0.59	0.03	1.24	1.73	0.10
33, 40, 43, 50	0.55	1.19	0.22	0.66	0.02	0.66
34, 39, 44, 49	0.64	0.13	0.50	1.16	5.79	0.94
35, 38, 45, 48	0.36	0.65	0.78	4.62	1.46	0.60
36, 37, 46, 47	0.05	2.73	0.96	1.18	3.11	0.09

[a]Each element contains the modal strain energy fraction shown in the columns under the heading Mode number.

where sw_j and sa_j are the weighted average SRF and average SRF, respectively, and σ_j is the standard deviation. The weighted average SRFs provide a useful means to isolate the true damage in the structure from the fake damage generated by the measurement errors. Once the location of damage is detected, the extent of damage is obtained from the corresponding average SRF.

Illustrative Example

The 10-bay planar truss structure[2] shown in Figs. 1 contains 51 truss members and 44 finite element DOF. The node and element numbers are marked in the figure. Each bay is a 5-m square with two diagonal members. In this example, several assumptions are made for the assessment of structural damage: 1) the mass and stiffness matrices of the undamaged structure are known and have been verified by test data; 2) the structural damage occurs in a fashion that the stiffness properties are changed but the mass matrix and the geometrical configuration remain unchanged; 3) the measured modes of the damaged system may be inaccurate due to measurement noise and modal parameter identification error; and 4) the measured mode shapes may be incomplete in the sense that the mode shape coefficients are available only at the test DOF of a modal survey. The location and extent of damage will be assessed with these data and assumptions.

Employing Eq. (2), the fractional modal strain energy distribution in the first six flexible modes is calculated and shown in Table 1. Because of the symmetry of the structure, a number of elements exhibit identical modal strain energy distribution. Table 1 indicates that the longerons are carrying most of the strain energy in these modes and the diagonals are carrying a smaller fraction. The battens are carrying none or a very small fraction depending on the modes. No strain energy distribution among the battens for modes 1, 2, 4, and 5 indicates that the battens in these modes are not undergoing elastic deformation. If stiffness changes occur due to the damage only among the battens, there will be no changes in the natural frequencies and shapes in these modes. Thus, the system identification algorithms will not be able to detect the damage in the battens with these modes. Modes 3 and 6 should be used for damage detection of the battens.

Damage Detection with Complete, Accurate Measured Modes

Assume that the first six exact flexible modes of the damaged structure at the finite element DOF are available for damage detection. Since there are 51 SRFs to be identified and the number of the test DOF is the same as the number of the finite element DOF, i.e., 44, the minimum number of modes to be used becomes two. For the sake of brevity, results obtained using 15 different combinations of two modes are reported here.

Several damage cases are examined. The first damage case is a 30% stiffness reduction of element 4 (a longeron at bay 4). The resulting SRFs obtained using each of the 15 sets of modes are all zero except $s_4 = -0.3$ detecting the 30% stiffness reduction accurately. The second damage case is a 30% stiffness reduction of a diagonal at bay 6 (element 37). With the same sets of modes, the damage is detected exactly. The third damage is a 30% stiffness reduction occurring at the batten between bay 8 and 9 (element 29). The results indicate that the accurate damage detection is possible only when the measured mode sets, including either mode 3 or mode 6, are used. When the combinations of modes 1, 2, 4, and 5 are used, the damage detection is not possible. The results are consistent with the observation made with the modal strain energy distribution of the undamaged structure. Modes 1, 2, 4, and 5 are not affected by the stiffness reduction of the batten and are unable to detect the damage. Finally, the three damage cases with 30% stiffness reduction are incorporated simultaneously. Accurate detection of the damage is possible with each of the 15 sets of modes.

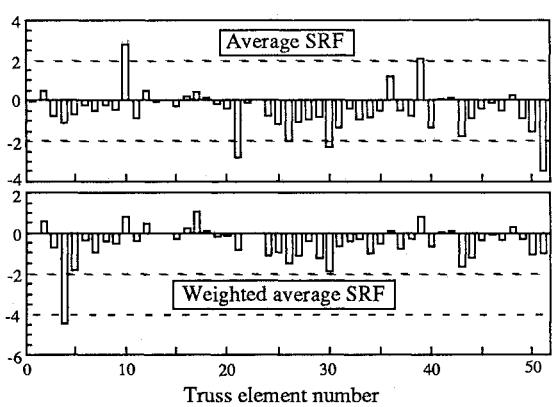

Fig. 2 Damage detection using a test analysis model.

Damage Detection with Incomplete, Inaccurate Measured Modes

The damage detection using the inaccurate mode shapes available only at test DOF is investigated here. From the truss structure in Figs. 1, 22 test DOF are selected; they include X DOF of all even node numbers and Y DOF of all odd node numbers. The mass and stiffness matrices and the submatrices in the finite element DOF are reduced to the test DOF using the modal reduction technique. The first six flexible modes are used to define the transformation matrix for the reduction and for the damage detection. The inaccurate measured mode shapes are simulated by multiplying each exact mode shape coefficient of the damaged structure by the factor $1 + \epsilon$, where ϵ is a random number with uniform probability between $\pm\beta$. To simulate a 20% noise level, β is set to be 0.2. Since there are 51 SRFs to be identified and the number of test DOF is 22, the minimum number of modes needed for damage detection becomes three. Twenty different combinations of three modes out of the six measured modes are used to assess the damage. The damage detection of the 100% reduction in elements 4, 29, and 37 is investigated. The average SRFs obtained using the 20 combinations are shown in Fig. 2. Meaningful damage detection appears to be difficult. To help find the true damage, the weighted average SRFs are evaluated and shown in the figure. The damage in element 4, which carries a large modal strain energy, is clearly visible. The corresponding average SRF is -1.12. The damage at elements 29 and 37 is not distinguishable from the other fake damages.

Concluding Remarks

A precise detection of damage location and extent was possible when a sufficient number of exact measured modes of a damaged structure in the finite element DOF was employed for damage detection. The evaluation of modal strain energy among the submatrices and modes of a undamaged structure provided useful information on how to select the modes for damage detection. The performance of the proposed method using inaccurate measured mode shapes in test DOF and a TAM was evaluated using a planar truss example. The identified SRFs varied significantly depending on the set of modes used for damage detection. In order to resolve this problem, an average SRF weighted by the standard deviation of the SRFs obtained using various sets of measured modes was proposed. The weighted average SRF helped to locate the true damage among the fake damage generated by the inconsistent measurements. The results indicated that damage at the elements containing a large portion of the modal strain energy among the modes used for damage detection would be most likely to be detected accurately.

References

[1]Chen, J.-C., and Garba, J. A., "On-Orbit Damage Assessment for Large Space Structures," *AIAA Journal*, Vol. 26, No. 9, 1988, pp. 1119-1126.

[2]Smith, S. W., and Hendricks, S. L., "Evaluation of Two Identifi-

cation Methods for Damage Detection in Large Space Trusses," *Proceedings of the Sixth VPI&SU/AIAA Symposium on Dynamics and Control of Large Structures*, Virginia Polytechnic Inst. and State Univ., Blacksburg, VA, June 1987, pp. 127-142.

[3]Hajela, P., and Soeiro, F. J., "Structural Damage Detection Based on Static and Modal Analysis," *AIAA Journal*, Vol. 28, No. 6, 1990, pp. 1110-1115.

[4]Lim, T. W., "A Submatrix Approach to Stiffness Matrix Correction Using Modal Test Data," *AIAA Journal*, Vol. 28, No. 6, 1990, pp. 1123-1130.

[5]Kammer, D. C., "Test-Analysis-Model Development Using an Exact Modal Reduction," *International Journal of Analytical and Experimental Modal Analysis*, Vol. 2, No. 4, 1987, pp. 174-179.

[6]Guyan, R. J., "Reduction of Stiffness and Mass Matrices," *AIAA Journal*, Vol. 3, No. 2, 1965, p. 380.

Improved Solution for Ill-Conditioned Algebraic Equations by Epsilon Decomposition

Irving U. Ojalvo*
University of Bridgeport, Bridgeport, Connecticut 06601

Nomenclature

(A)	$= n \times n$ symmetric matrix
$(\bar{A})$	= matrix (A) with ϵ added to diagonal elements
$\{b\}$	= right-hand side of simultaneous algebraic equations
$\{c\},\{\bar{c}\}$	= coefficient vectors for eigenvector expansion of $\{x\}$ and $\{\bar{x}\}$
c_i	= elements of $\{c\}$
$K(A)$	= spectral condition number of (A)
p	= number of zero and near-zero eigenvalues
r	= rank of (A)
$\{x\}$	= solution vector
$\{\bar{x}\}$	= E-D solution before improvement
$\{x_{ED}\}$	= E-D solution after improvement
$\{\beta\}$	= coefficient vector for eigenvector expansion of $\{b\}$
β_i	= elements of $\{\beta\}$
ϵ	= small parameter used in E-D
(Λ)	= diagonal matrix of eigenvalues of (A)
λ_i	= eigenvaue of (A)
$\bar{\lambda}_i$	= eigenvalue of $(\bar{A})$
(Φ)	= matrix of eigenvectors of (A)
$\{\phi_i\}$	= eigenvector of (A)

Introduction

LINEAR algebraic equations with rank deficiency, which are characterized by zero eigenvalues and zero determinants, do not have unique mathematical solutions. Unfortunately, an a priori knowledge of system rank deficiency is not always available, and parameter estimation techniques used in system identification often generate ill-conditioned equations. This can cause anomalous and highly sensitive results, even when special care is taken during the numerical solution process. Such sensitivity is characterized by the fact that small perturbations of the right-hand side or the coefficient matrix (perhaps caused by physical measurement error or limited numerical computation precision) can produce widely varying solutions.

In this Note, matrix eigenvalue theory is used to examine the source of ill conditioning in linear algebraic equations. This approach highlights the crucial role played by the zero and near-zero eigenvalues and corresponding eigenvectors of poorly conditioned systems. Insight gained from this approach is used to significantly improve a recently developed solution procedure called epsilon decomposition (E-D).[1,2] The efficiency of the improved E-D over singular value decomposition (SVD)[3,4] resides in the need to only obtain the zero and near-zero eigenvalues of the coefficient matrix as opposed to all its eigenvalues and vectors (as required by SVD). Thus the efficiency of E-D is significant for large matrices with small rank deficiency.

Technical Background

Given a symmetric set of linear algebraic equations

$$(A)\{x\} = \{b\} \tag{1}$$

where

$$(A) = (A)^T \tag{2}$$

Although an eigenvector solution approach for Eq. (1) is not advocated, it will be useful for future discussions to consider the eigenstructure of (A), $\{x\}$, and $\{b\}$. Therefore, let $\{\phi_i\}$ $i = 1, 2,\ldots, n$ be the orthonormal solutions to

$$(A)\{\phi_i\} = \lambda_i\{\phi_i\} \tag{3}$$

and since (A) is symmetric

$$\begin{aligned} \{\phi_i\}^T\{\phi_j\} &= 0 \qquad i \neq j \\ &= 1 \qquad i = j \end{aligned} \tag{4}$$

Defining the totality of eigenvectors and eigenvalues of Eq. (3) by (Φ) and (Λ), respectively, Eqs. (3) and (4) may be rewritten as

$$(A)(\Phi) = (\Phi)(\Lambda) \tag{5}$$

$$(\Phi)^T = \Phi^{-1} \tag{6}$$

where (Λ) is the diagonal matrix of eigenvalues and the columns of (Φ) are the eigenvectors $\{\phi_i\}$.

Alternate pre- and postmultiplication of Eq. (5) by $(\Phi)^T$ and (Φ), respectively, results in the relationships

$$(\Phi)^T(A)(\Phi) = (\Lambda) \tag{7}$$

$$(A) = (\Phi)(\Lambda)(\Phi)^T \tag{8}$$

whereas eigenexpansion of $\{x\}$ and $\{b\}$ yields

$$\{x\} = (\Phi)\{c\} = \Sigma c_i\phi_i \tag{9}$$

$$\{b\} = (\Phi)\{\beta\} = \Sigma\beta_i\phi_i \tag{10}$$

where $c_i = \{\phi_i\}^T\{x\}$ and $\beta_i = \{\phi_i\}^T\{b\}$.

Substitution of Eqs. (9) and (10) into Eq. (1) and use of Eqs. (6-8) yields

$$(\Lambda)\{c\} = \{\beta\}$$

or

$$\lambda_i c_i = \beta_i \tag{11}$$

Received Jan. 25, 1990; revision received Aug. 13, 1990; accepted for publication Oct. 4, 1990.

*Bullard Professor, Mechanical Engineering Department; currently Senior Research Scientist and Adjunct Professor of Engineering Mechanics, Columbia University, New York, NY 10027. Member AIAA.